Center for Turbulence Research
Proceedings of the Summer Program 1994

Triple flame structure and diffusion flame stabilization

By D. Veynante,[1] L. Vervisch,[2] T. Poinsot,[3] A. Liñán[4] AND G. Ruetsch[5]

The stabilization of diffusion flames is studied using asymptotic techniques and numerical tools. The configuration studied corresponds to parallel streams of cold oxidizer and fuel initially separated by a splitter plate. It is shown that stabilization of a diffusion flame may only occur in this situation by two processes. First, the flame may be stabilized behind the flame holder in the wake of the splitter plate. For this case, numerical simulations confirm scalings previously predicted by asymptotic analysis. Second, the flame may be lifted. In this case a triple flame is found at longer distances downstream of the flame holder. The structure and propagation speed of this flame are studied by using an actively controlled numerical technique in which the triple flame is tracked in its own reference frame. It is then possible to investigate the triple flame structure and velocity. It is shown, as suggested from asymptotic analysis, that heat release may induce displacement speeds of the triple flame larger than the laminar flame speed corresponding to the stoichiometric conditions prevailing in the mixture approaching the triple flame. In addition to studying the characteristics of triple flames in a uniform flow, their resistance to turbulence is investigated by subjecting triple flames to different vortical configurations.

1. Introduction

The structure and the stabilization of diffusion flames is a topic of intense research which has numerous practical applications in jet flames, aircraft engines, diesel car engines, torches, etc. At the same time, it is a complex phenomenon which has generated much theoretical and experimental work in the last years (Takahashi *et al.* 1990, Liñán 1994, Dold 1989, Kioni *et al.* 1993).

Our goal in the present work is to investigate two aspects of diffusion flame stabilization as suggested from asymptotic theory: (1) stabilization of a diffusion flame in the viscous region immediately downstream of the flame holder, and (2) stabilization of the diffusion flame as a triple flame far downstream.

These two computations are performed for laminar flows only: the triple flame is considered in Section 4 while the stabilization at the splitter plate is studied

1 Laboratoire EM2C, Ecole Centrale Paris, France
2 LMFN/INSA CORIA/URA CNRS230 Rouen France
3 Institut de Mecanique des Fluides de Toulouse and CERFACS, France
4 E.T.S.I. Aeronáuticos, Universida Politecnica de Madrid
5 Center for Turbulence Research

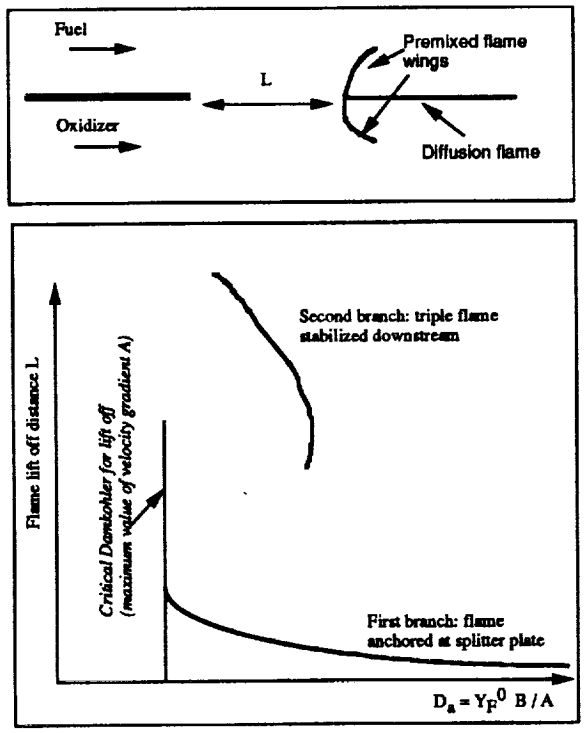

FIGURE 1. Asymptotic results for diffusion flame stabilization and lift-off.

in Section 5. The influence of turbulence is investigated later in Section 6 by using a technique developed previously for premixed flames both experimentally and numerically (Roberts *et al.* 1993, Samaniego 1993, Poinsot *et al.* 1991): vortices are generated upstream of the flame and interact with the flame front. Although these isolated vortices are too crude to represent real turbulence, they provide useful estimates of the effects of hydrodynamic excitation on the flame and of the flame's capacity to resist these excitations.

2. Regimes of flame stabilization

Classical results concerning triple flame studies may be found in Dold 1989, Liñán 1988, Dold *et al.* 1991, and Liñán and Crespo 1976. For the present study we have chosen to focus on two aspects of triple flame stabilization: stabilization in the wake of the splitter plate (anchored case) or stabilization far downstream (lifted flame). These two aspects correspond to the two stable branches of the curve proposed by Liñán (1994) and given in Fig. 1. The x coordinate corresponds to the Damköhler number defined by $D_a = Y_O^0 B/A$ where B is the pre-exponential constant and A is the velocity gradient at the splitter plate. The y coordinate is the distance between the flame holder and the flame.

The lower branch of Fig. 1 corresponds to flames stabilized in the wake of the splitter plate. When the velocity gradient in the wake increases, the flame moves

slightly downstream until a critical value of the velocity gradient, A_{lo}, is reached. At that point, flame stabilization is no longer possible near the splitter plate and the flame is lifted off. The critical value at which lift off occurs is estimated by Liñán as

$$Y_O^0 B/A_{lo} = \Phi^3 \exp(\Phi) \tag{1}$$

where Φ is a nondimensional parameter defined by

$$\Phi = \frac{T_a}{T_0}\left(1 + \frac{QY_F^0}{c_P T_0(1 + rY_F^0/Y_O^0)}\right)^{-1}$$

In these equations, T_a is the activation temperature, Q is the heat released per unit mass of fuel, and $r = (W_O\nu_O)/(W_F\nu_F)$ or the mass ratio of oxidizer to fuel in the reaction. We will check in Section 5 whether numerical simulations confirm this analysis.

If lift-off occurs, then stabilization may occur downstream of the splitter plate (on the upper branch of Fig. 1) if the local flow speed decreases enough to be equal to or less than the characteristic triple-flame speed which may exist at that point. In this case, the local velocity profile upstream of the flame is essentially constant (initial shear has been dissipated), and the problem may be viewed as an eigenvalue problem in which a triple flame propagates at a constant speed in a flow which is moving in the opposite direction at the same absolute speed. Numerically, it is essential to be able to track in real time the value of this velocity to keep the flame inside the computational box. When the triple flame is stabilized, it is possible to study its structure and propagation speed. Asymptotic studies suggest that triple flames may propagate at a speed U_F larger than the premixed flame speed S_L^0 corresponding to the conditions encountered at the tip of the triple flame.

3. Numerical method and configurations

For all computations presented here, the fully-compressible reacting Navier Stokes equations were solved in two dimensions. The chemistry used corresponds to a simple irreversible reaction:

$$\nu_F F + \nu_O O \rightarrow \nu_P P$$

and the mass reaction rate for the fuel F is written following Williams (1985):

$$\dot{\omega}_F = D\nu_F W_F/Y_F^0 \rho^{ex}(Y_F/W_F)^{\nu_F}(Y_O/W_O)^{\nu_O}\exp(-T_a/T) \tag{2}$$

where T_a is the activation temperature.

For simplicity, the stoichiometric coefficients ν_O and ν_F have been set to unity in this study. Two values of ex have been used (1 and 2). For both cases, to allow comparison with asymptotic results, Eq. (2) may be written

$$\dot{\omega}_F = B\rho^{ex} Y_F Y_O exp(-T_{act}/T) \tag{3}$$

where B has the dimension s^{-1} if $ex = 1$ and $m^3/(kgs)$ if $ex = 2$.

Using this formulation for the reaction rate, the conservation equations to be solved are:

$$\frac{\partial \rho}{\partial t} + \frac{\partial}{\partial x_i}(\rho u_i) = 0$$

$$\frac{\partial \rho u_i}{\partial t} + \frac{\partial}{\partial x_j}(\rho u_i u_j) = -\frac{\partial P}{\partial x_i} + \frac{\partial \tau_{ij}}{\partial x_j}$$

$$\frac{\partial \rho E}{\partial t} + \frac{\partial}{\partial x_i}[(\rho E + P)u_i] = \frac{\partial}{\partial x_i}(\tau_{ij}u_j) + \frac{\partial}{\partial x_i}\left(\lambda \frac{\partial T}{\partial x_i}\right) + Q\dot{\omega}_F$$

$$\frac{\partial \rho Y_F}{\partial t} + \frac{\partial}{\partial x_j}(\rho Y_F u_j) = \frac{\partial}{\partial x_i}\left(\rho \mathcal{D}_F \frac{\partial Y_F}{\partial x_i}\right) - \dot{\omega}_F$$

$$\frac{\partial \rho Y_O}{\partial t} + \frac{\partial}{\partial x_j}(\rho Y_O u_j) = \frac{\partial}{\partial x_i}\left(\rho \mathcal{D}_O \frac{\partial Y_O}{\partial x_i}\right) - r\dot{\omega}_F$$

where the total energy density and deviatoric stress tensor are given by:

$$\rho E = \frac{1}{2}\rho u_i^2 + \frac{P}{\gamma - 1}$$

$$\tau_{ij} = \mu\left(\frac{\partial u_i}{\partial x_j} + \frac{\partial u_j}{\partial x_i} - \frac{2}{3}\delta_{ij}\frac{\partial u_k}{\partial x_k}\right)$$

We assume that the mixture has a specific heat ratio of $\gamma = 1.4$ and the dynamic viscosity is a function on temperature, $\mu = \mu_0(T/T_0)^b$, with $b = 0.76$. We also assume that the Prandtl and Schmidt numbers,

$$Pr = \frac{\mu c_p}{\lambda}; Sc = \frac{\mu}{\rho \mathcal{D}},$$

remain constant, and $\mathcal{D} = \mathcal{D}_F = \mathcal{D}_O$. As a result, the Lewis number $Le = Sc/Pr$ is constant and is taken as unity throughout this study. We can also define the heat release parameter and Zel'dovich numbers as:

$$\alpha = \frac{T_f - T_0}{T_f}; \beta = \alpha \frac{T_a}{T_f}$$

where T_f is the adiabatic flame temperature.

The governing equations are solved using direct numerical simulations. Spatial derivatives are taken using sixth-order compact difference algorithm of Lele 1990, and time advancement is performed using a third-order Runge Kutta scheme (Wray 1990). Boundary conditions are specified using the Navier-Stokes characteristic boundary condition method of Poinsot and Lele 1990.

4. Characteristics of a lifted triple flame

We begin the analysis of triple flames by considering a lifted triple flame stabilized in the far field with a uniform inflowing velocity. In addition to describing the stabilization in the lifted case, this approach can be viewed as a first step in understanding the behavior of triple flames in more complicated flow scenarios, such as in the wake of a splitter plate (section 5) and in response to vortices (section 6).

We initialize the computations of the triple flame by first stabilizing a planar premixed flame in the computation domain. In doing so, the mixture fraction is uniform throughout the domain with the stoichiometric value $Z = Z_S = 0.5$. Associated with this flame are the planar flame speed S_L^0 and the planar flame thickness δ_L^0. We then change the inflow mixture fraction profile from uniform to a hyperbolic tangent profile varying from $Z = 0$ to 1 while maintaining the same uniform inlet velocity profile. The response of the flame to the mixture fraction gradient is shown in the time sequence of Fig. 2. For this case the heat release corresponds to $\alpha = 0.75$ and the Zel'dovich number is $\beta = 8.0$. With the uniform flow approaching from the left, as the mixture fraction gradient reaches the flame surface only the centerline is exposed to the stoichiometric mixture fraction and locally maintains the planar flame speed and reaction rate. Above this point the mixture is fuel rich, and below fuel lean. As a result, these regions of non-unity equivalence ratio burn less, the reaction rate drops, and the local flame speed is reduced. The excess fuel and oxidizer then combine behind the premixed flame along the stoichiometric surface and burn in a trailing diffusion flame. Thus the "triple" flame refers to the fuel-rich premixed flame, the fuel-lean premixed flame, and the trailing diffusion flame.

4.1 Flame stabilization

In addition to the change in structure that occurs when the planar premixed flame is subjected to a mixture fraction gradient, the propagation velocity of the flame increases, as observed in Fig. 2. In order to study the triple-flame in further detail, a method of stabilizing the flame in the computational domain is needed. We accomplish this by calculating the relative progression velocity of iso-scalar surfaces. This method, also used in Vervisch *et al.* 1994, results from equating the transport equation for a scalar variable Y:

$$\rho\frac{DY}{Dt} = \frac{\partial}{\partial x_i}\left(\rho\mathcal{D}\frac{\partial Y}{\partial x_i}\right) + \dot{w}_Y$$

with the Hamilton-Jacobi equation for the scalar field (Kerstein *et al.* 1988):

$$\rho\frac{DY}{Dt} = \rho V|\nabla Y|.$$

Solving for the relative progression velocity, V, we obtain:

$$V = \frac{1}{\rho|\nabla Y|}\frac{\partial}{\partial x_i}\left(\rho\mathcal{D}\frac{\partial Y}{\partial x_i}\right) + \frac{1}{\rho|\nabla Y|}\dot{w}_Y$$

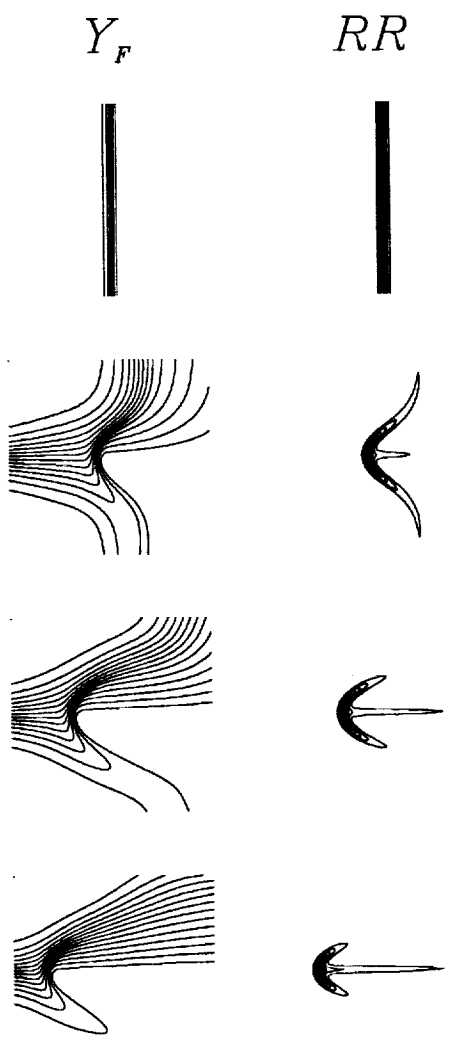

FIGURE 2. Response of a planar premixed flame to a mixture fraction gradient. The top row shows the flame under premixed conditions, with a uniform flow approaching from the left. As the mixture fraction gradient reaches the flame surface, the flame shape changes from a premixed planar flame to one with fuel-rich and fuel-lean premixed curved fames followed by a trailing diffusion flame. In addition to the change in shape, the flame propagates faster relative to the premixed case.

This relation is evaluated on the centerline in the preheat zone and subtracted from the local fluid velocity, giving the correction to be applied at the inlet. If one were to apply this correction at the inlet alone, then changes to the flame would only

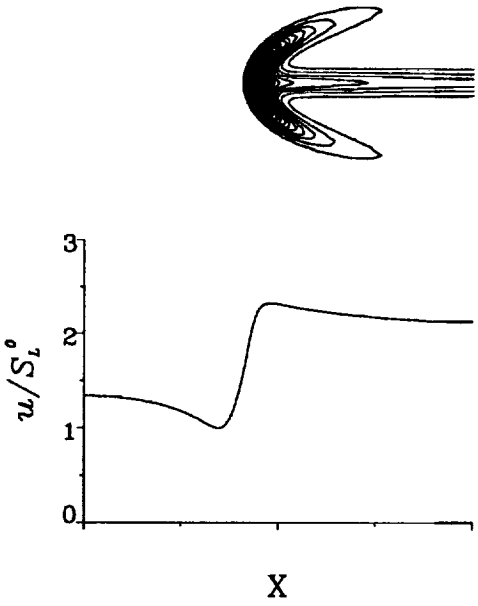

FIGURE 3. Reaction rate and horizontal velocity along the centerline.

occur after the convective time required to reach the flame, which is both time consuming and can also introduce stability problems. A more efficient method is to apply the correction to all points in the flow, as a Gallilean transformation, such that the steady state situation is quickly reached.

4.2 Effect of heat release

We now turn our attention to studying the effect of heat release on the triple flame and, in particular, how this affects the propagation velocity. The analytical work of Dold 1989 and Hartley and Dold 1991 provide estimates of the triple-flame speed for weak ($\beta\partial Z/\partial y \to 0$) and moderate ($\beta\partial Z/\partial y \sim O(1)$) values of the mixture fraction gradient under the assumption of zero heat release. They find that the flame speed is greatest for zero mixture fraction gradient, corresponding to a planar flame, and then decreases as the mixture fraction gradient increases. This is in contrast to the change in flame speed we observe in Fig. 2. The discrepancy lies in the assumptions concerning heat release. To investigate this further, we examine the velocity field along the centerline of the triple flame in Fig. 3. Here we observe that, in addition to the rise in velocity through the flame, the horizontal component of the velocity reaches a minimum before the flame. The velocity at this minimum is close to the planar laminar flame speed, and far upstream the velocity is larger. Therefore it is necessary to distinguish these two velocities. The local flame speed is important in terms of chemical reaction, where the far-field flame speed is identified with the propagation of the entire structure, U_F.

The mechanism responsible for this velocity difference can be seen in the sketch of Fig. 4. Here we examine the velocity vectors before and after they pass through

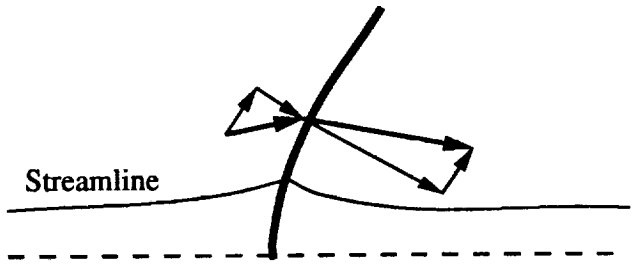

FIGURE 4. Mechanism responsible for creating triple-flame speeds larger than the planar-flame speeds. Heat release causes an increase in the normal component of flow, and the flow redirection causes an upstream divergence of flow.

the flame surface. In cases where there is heat release, the component of the velocity perpendicular to the flame increases across the surface, whereas the tangential component remains unchanged. The jump in the perpendicular velocity component results in a bending of the velocity vector towards the centerline. This redirection of the flow is accommodated by the divergence of the stream lines ahead of the flame, resulting in the decrease of the velocity observed in Fig. 3. Since the local flame speed along the stoichiometric line is S_L^0, the flame can be stabilized only if the flow speed at this point remains near S_L^0, which requires an increase in the upstream velocity. Note than in absence of heat release, there is no flow redirection across the flame and therefore the far-field and local flame speeds are equal.

4.3 Effect of the mixture fraction gradient

In their previous analytical work, Dold 1989 and Hartley and Dold 1991 observed a large effect of the mixture fraction on the triple-flame speed. Due to the effects of flame curvature, they observed a decrease in the flame speed as the mixture fraction gradient increases and thus radius of curvature decreases. In cases with heat release, we observe qualitatively the same behavior although the quantitative aspects are very different. For zero heat release cases the planar premixed flame is an upper limit for the flame speed; however, for finite heat release the flame speed is always observed to be greater than S_L^0. This is depicted in Fig. 5, where the far-field flame speed, U_F/S_L^0, and the local flame speed are plotted versus the inverse of the mixture fraction gradient taken at the flame location, $(\delta_L^0 \partial Z/\partial y)^{-1}$, representing a mixing layer thickness or alternatively a Damköhler number. Here we see that, in agreement with the zero heat release analysis, the local flame speeds remain of the order of S_L^0, decreasing slightly below this value for small values of the mixing thickness.

For small values of the mixing thickness, one might expect quenching to occur. However, in agreement with the analysis of Dold 1989 and Hartley and Dold 1991, quenching is not observed. Under the assumption of zero heat release, quenching was observed only when the flame was subjected to an external strain(Dold *et al.* 1990). In cases with heat release, the resistance to quenching is further strengthened. The

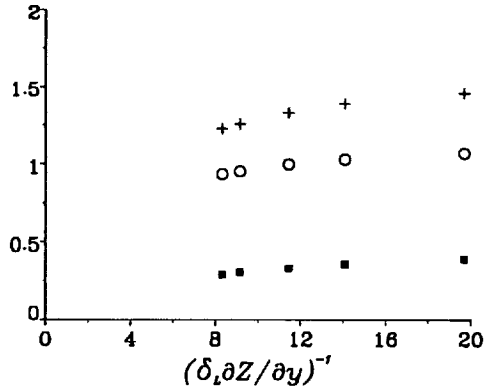

FIGURE 5. Far-field flame speed(+), local flame speed(o), and their differences(■) as a function of the mixing thickness. All speeds are normalized by S_L^0, and for all cases $\alpha = 0.75$ and $\beta = 8.0$. The mixture fraction gradient is evaluated along a line passing through the maximum reaction rate.

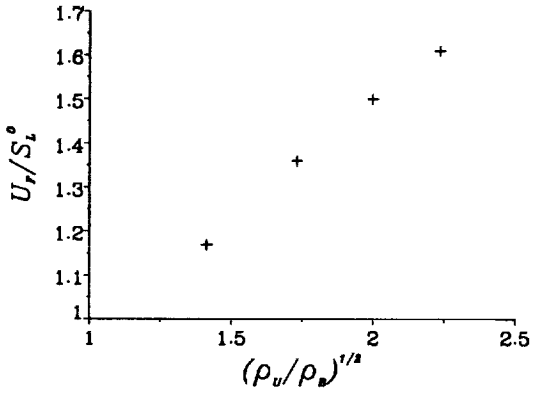

FIGURE 6. Ratio of triple-flame to planar-flame speeds for various heat releases.

strain field which creates the reduction in the horizontal velocity also decreases the effective mixture fraction gradient in front of the flame, and therefore limits how small the effective Damköhler number can become in Fig. 5. The only way to continue this graph to smaller thicknesses is to apply a strain of opposite sense externally, (*cf.* Section 6 where the response of triple flames to vortices is examined).

As the mixing thickness increases, not only do the far-field and local flame speeds increase, but also the difference between the two, indicating that heat release effects become more important as the mixture thickness increases. This trend can be understood by applying the mechanism in Fig. 3 to different mixing thicknesses. Since the difference between the far-field and local flame speeds depends on the flow redirection through the flame, which *locally* depends on the reaction rate along

the premixed wings, then the distribution of the reaction rate along the premixed wings becomes an important characteristic. As the mixing thickness becomes larger, the reaction rate is stronger along the premixed wings as one moves away from stoichiometric conditions. This causes the flow to be deflected more and thus the difference in the velocities to increase.

In the limit of large mixing thickness, one expects from asymptotic results that the flame speed reaches a constant value for a given heat release. This value is related to the jump in density by:

$$\frac{U_F}{S_L^0} \sim \sqrt{\frac{\rho_u}{\rho_b}}$$

A comparison of data from numerical simulations with this result is shown in Fig. 6, where overall good agreement is observed.

5. Diffusion flame stabilized in the wake of a splitter plate

5.1 Configuration and parameters

In the region immediately downstream of the splitter plate, the velocity profile exhibits a wake which has a strong influence on flame stabilization. For this work, we assume that both streams have the same speed and vorticity thickness so that the velocity gradient at the splitter plate, A, is the same on both sides of the plate. Inlet profiles for temperature, species, and velocities are given in Fig. 7; the temperature is imposed everywhere and equal to the splitter plate temperature, and species profiles correspond to step functions.

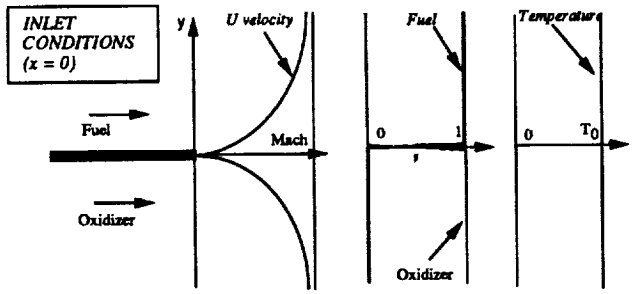

FIGURE 7. Configuration for simulations of diffusion flame stabilization lift-off

For these computations it is important to control inlet temperature; asymptotic analysis shows that flame stabilization is obtained not only from the existence of a low velocity region in the wake, but also from the presence of heat losses from the flame to the splitter plate.

The parameters controlling the flow are the Mach number at infinity (equal on both sides) $M_a = U_o/c$ and the width of the shear layers δ. The characteristic velocity gradient A is $A = U_o/\delta$. The velocity profile at the inlet was chosen in different ways depending on the runs: (1) a *tanh* profile was first used, where $u(y) = U_o tanh(y/\delta)$. This profile leads to a singular point at $y = 0$ and sometimes to numerical instabilities; (2) an *exp* profile was also tested where $u(y) = U_o(1 - exp(-y^2/\delta^2))$. Corresponding runs will be labeled as 'tanh' or 'exp' cases. For all cases, the reference Reynolds number cL/ν is 1000 where L is the reference length of the problem, ν is the kinematic viscosity in the fuel at infinity, and c is the sound speed in the fresh gases. The parameters controlling the chemistry for these runs are given in Table 1.

Table 1. Chemistry parameters for DNS of triple flame in a wake

Case	T_{act}/T_0	T_a/T_0	D_{fuel}	b	Pr	Le	S_L^0/c	d/L	δ_l^0/L
Flame 1	18	5	53	0.76	0.75	1.0	0.022	0.046	0.4
Flame 2	12	5	53.	0.76	0.75	1.0	0.08	0.013	0.16

The adiabatic temperature T_a and the laminar flame speed S_L^0 given above correspond to a premixed laminar flame speed where the premixed gases would have a fuel mass fraction equal to $Y_F^0/2$ and an oxidizer mass fraction of $Y_O^0/2$. These levels are the maximum levels which may be obtained in the wake of the splitter plate, and therefore this velocity is the maximum premixed flame speed which may exist in the wake. The Lewis number is the same for oxidizer and fuel, and the problem is symmetric ($Y_F^0 = Y_O^0 = 1$). Molecular weights are also supposed to be equal, and in the expression of the reaction rate, ex is 2. The reduced pre-exponential constant D_{fuel} is defined by $D_{fuel} = \nu_F LB\rho_0 Y_O^0/(cW)$ where W is the molecular weight of fuel or reactant. The two flame thicknesses indicated are $d = \nu/S_L^0$ and $\delta_l^0 = (T_a - T_0)/Max(\frac{\partial T}{\partial x})$.

5.2 Structure of stabilized diffusion flames

Let us first consider a stabilized triple flame in a wake. For this case, the parameters are a Mach number of 0.2, a vorticity thickness of 0.05 with an *exp* profile, and chemistry parameters corresponding to Flame 2 (see Table 1). In this case, a stabilized flame is found in the wake at a distance D which is given by $D/L = 0.95$ (or $D/d = 73$ or $D/\delta_l^0 = 5.9$). The density field (similar to the temperature field) and the reaction rate field are given in Fig. 8. The influence of the cold splitter plate is clearly seen from the density field. The flame is losing energy towards the plate, and this phenomenon produces flame stabilization. Without the plate the flame would propagate even more upstream and eventually get stabilized on the

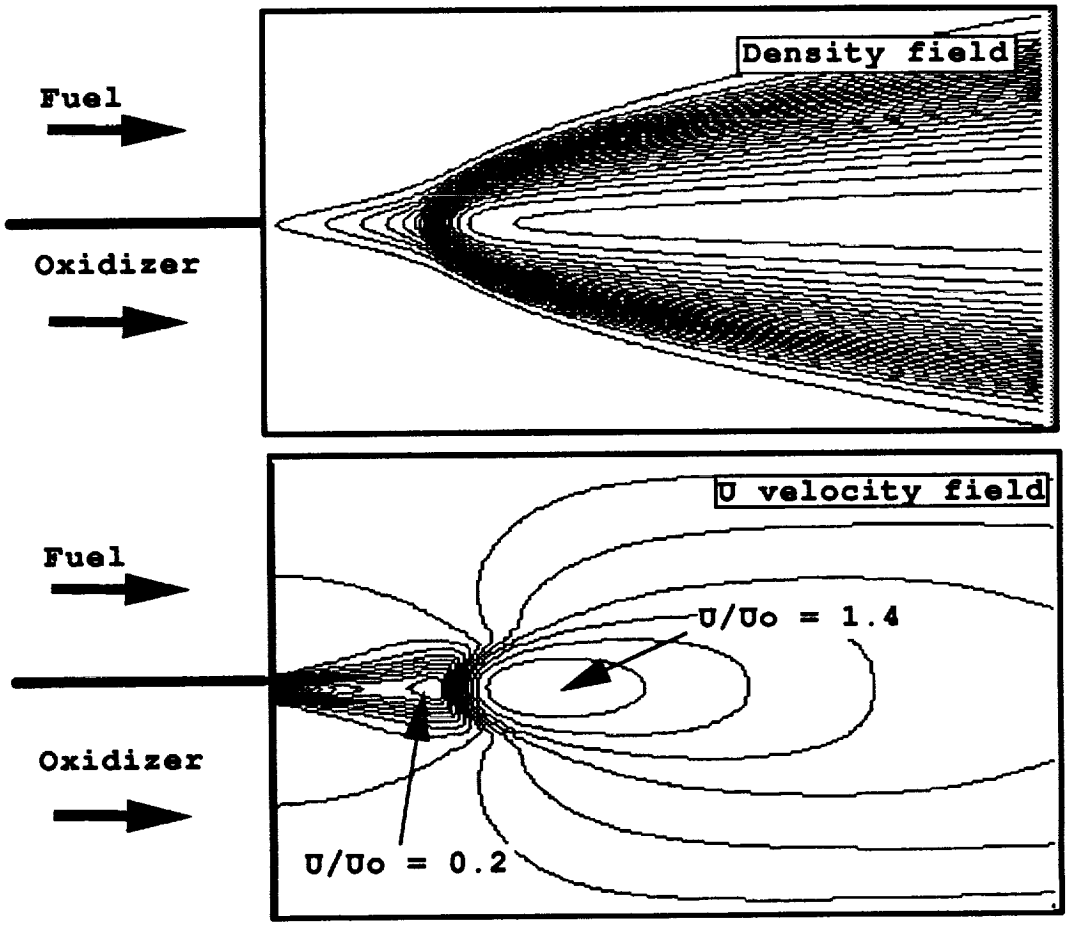

FIGURE 8. Triple flame stabilized in a wake.

splitter plate. This situation would not be unusual but we wanted to avoid it for the first test cases.

Different cuts along the centerline axis of the flame (Case 15) are presented in Fig. 9. The axial velocity profile is plotted along with the same profile in the case without the flame (wake only). It is seen that for small values of x, both profiles are essentially similar (close to the splitter plate). For larger x values, the influence of the triple flame on the flow divergence is first felt and the velocity decreases for the triple flame while the cold flow velocity keeps increasing. Finally closer to the flame front, a second effect due to the flame appears: temperature starts increasing, the density decreases, and the velocity increases to a value of the order of $1.4U_o$.

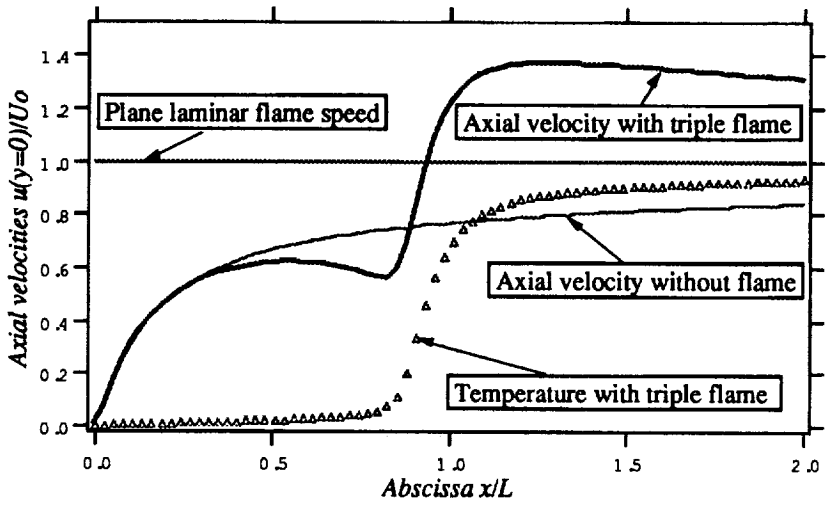

FIGURE 9. Axial velocity and temperature profiles along wake axis.

5.3 Stability domain of the diffusion flame in a wake flow

An important question for practical applications is the possibility of predicting flame stabilization. For triple flames, the usual technique used for this prediction is to compare the local flow speed and the triple flame speed. Stabilization may be obtained if the local flow speed is smaller than the flame speed.

DNS results as well as asymptotic theory provides a slightly more complex picture. Fig. 10 compares plots of axial velocity along the wake axis for three stabilized triple flames (Cases 13, 15, and 16) and one lifted flame (Case 19) with the propagation speed of the triple flame. When doing this exercise, one has to take into account the decrease of the flame speed to zero when the flame comes too close to the splitter plate. This phenomenon explains how a 'stable' stabilization point may be obtained in a triple flame. If heat losses towards the splitter plate are not accounted for, the local flow speed will always be less than the flame speed near the splitter plate, and this theory will always predict stabilization close to the splitter plate. It is therefore crucial to include heat losses effect into the evaluation of the flame speed U_F. This was done here in a crude way using the following formula:

$$U_F = U_P(1 - exp(-\frac{D - P_1 d}{P_2 d})) \tag{4}$$

where P_1 and P_2 are two Peclet numbers and D is the stand-off distance between splitter plate and flame. When $D < P_1 d$, no flame can exist. Furthermore, the influence of the wall is felt down to a distance of the order of $(P_1 + P_2)d$ (such relations may be found in studies of flame wall interaction and they were used here as a first guess of splitter plate effects). Typical values for P_1 and P_2 are 4. The quantity U_P is the triple flame speed determined in the previous section. It is proportional to S_L^0 but is larger due to flow divergence. For the present computation,

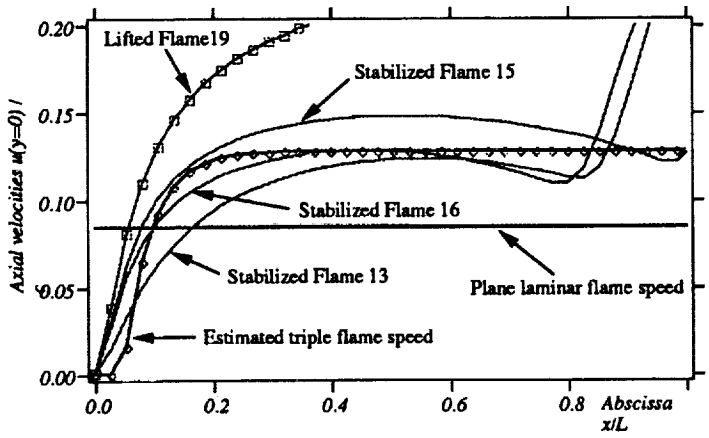

FIGURE 10. Velocity and temperature profiles along wake axis for different stabilized diffusion flames.

the following formula was used: $U_P = 1.5S_L^0$ as suggested from the study of the freely propagating triple flame studied above.

Fig. 10 shows that stabilization is indeed obtained if the flow speed on the wake axis U is at some point equal to U_F. For the lifted flame (Case 19), this is satisfied nowhere; the flame cannot find a stable location in the wake and it is lifted. Note that at the flame location itself, the local flow speed reaches a minimum as for free triple flames. However, this value of velocity is larger than the laminar unstrained flame speed. This is different from the "free" triple flame described above.

As for the freely propagating triple flame, the flow speed itself is strongly influenced by the flame. This influence may be evidenced by plotting the velocity difference on the wake axis between the reacting case and the cold flow case (Fig. 11). The triple flame induces a flow deceleration ahead of it. This deceleration scales with the laminar flame speed and may be compared to the result obtained for freely propagating flames in the previous sections.

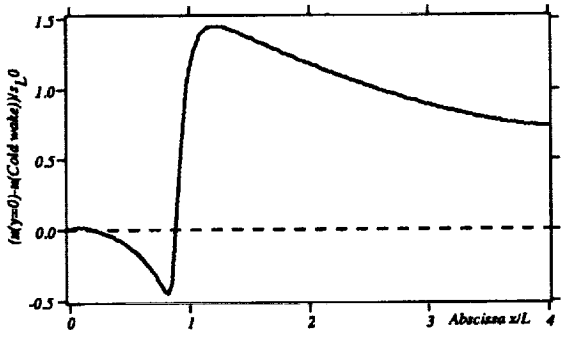

FIGURE 11. Velocity difference along wake axis between stabilized flame and cold flow cases.

From the above results, it is clear that in the configuration studied here, the velocity gradient is not the only controlling parameter for flame stabilization as suggested by asymptotic analysis. The velocity at infinity U_0 is also important. If this velocity is too small, we are too far from the assumptions of asymptotic analysis (where the velocity gradient is supposed to be maintained from $y = 0$ to $y = \infty$). For example, in the extreme case where the velocity U_0 is less than the flame speed S_L^0, the flame will always be stabilized independently of the velocity gradient A. However, for sufficiently large values of U_0, the velocity gradient A is indeed the controlling parameter. Lift off values of A were determined in these conditions for the two flames studied here by a process of trial and error. Results are given below. Since the asymptotic theory was developed with $ex = 1$, there is some uncertainty due to a slightly different expression of the reaction rate. Values of the parameters required to obtain lift off are also indicated (subscript $_{lo}$) both in code units and in flame units.

Table 2. Values of velocity gradient at liftoff

Flame	$A_{lo}L/c$	$A_{lo}L/c$	$\frac{S_L^0/\delta_l^0}{L/c}$	$\frac{A_{lo}}{(S_L^0/\delta_l^0)}$	$\frac{U_{o(lo)}}{c}$	$\frac{\delta_{lo}}{L}$	$\frac{U_{o(lo)}}{S_L^0}$	$\frac{\delta_{lo}}{\delta_l^0}$
	DNS	Asymp						
1	0.17	0.3	0.055	3.1	0.1	0.6	4.54	1.5
2	8	3.4	0.5	16	0.3	0.04	3.75	0.08

It appears that the trends provided by asymptotic analysis are correct but that the exact numbers are not right as expected from the differences between the asymptotic model and the actual computation. Flame 2 which has a lower activation temperature is much more difficult to lift than Flame 1. The normalized velocity gradient $A_{lo}L/c$ for lift off of Flame 2 is 47 times larger than the velocity gradient necessary to lift Flame 1. Asymptotic theory (developed in the limiting case of high activation energies) predicted an increase of 11 (instead of 47).

6. Interaction between vortical structures and triple flames

The triple-flame structure certainly plays an important role in turbulent combustion systems, for instance in the case of ignition of non-uniform mixtures it has been observed, through direct numerical simulation (Réveillon *et al* 1994), that triple flames traveling along the stoichiometric line may strongly contribute to the success of ignition. The triple flame then propagates in a turbulent environment, the stoichiometric line is distorted by the turbulence, and the flame is subjected to multiple interactions with vortical structures.

In this section, attention is focused on the interaction between the stabilized triple flame in the "far field" and a single vortex or a pair of vortices. Vortices are

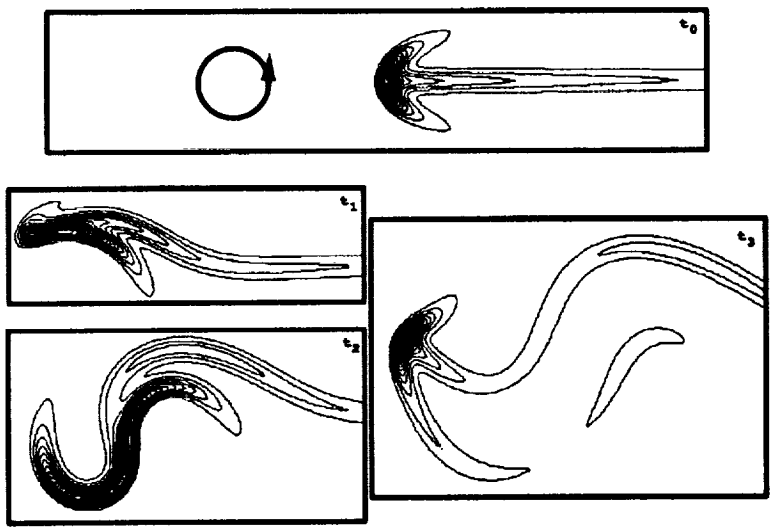

FIGURE 12. Triple flame interacting with a single vortex. Isocontours of the reaction rate are shown at three different times.

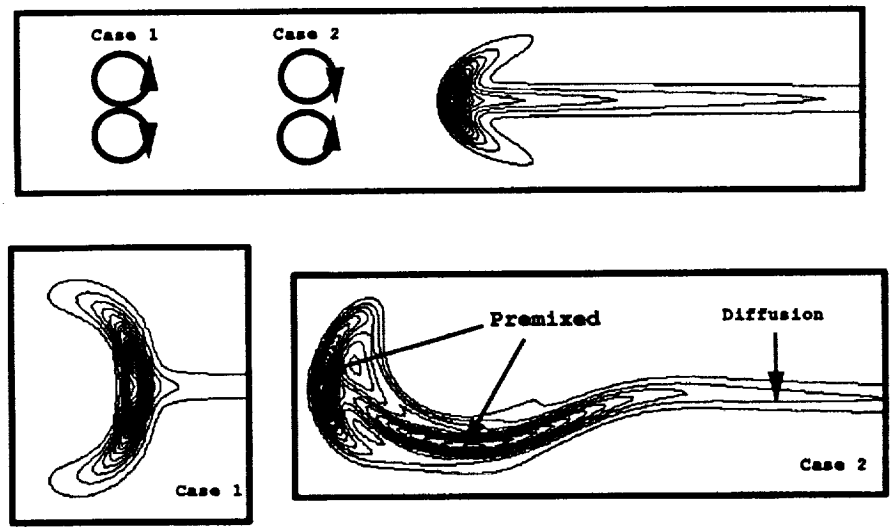

FIGURE 13. Triple flame interaction with two vortex pairs.

characterized by their maximum velocity, u_{vort}, and a length scale, δ_{vort}, chosen equal to the diameter of the single vortex or to the sum of the diameter and of the distance between the core of the vortices. Calculations have been realized for $u_{vort}/S_L^0 = 10$ and $\delta_{vort}/\delta_L^0 = 5$.

When either a single vortex or a pair of vortices proceed towards the triple flame, the mixture fraction field is convected by this vortical structure. Moreover, a distribution of strain rate is imposed to the diffusive and reactive layers and the resulting

velocity and species fields may strongly differ from those required to stabilize the flame. However, it is observed in Figs. 12 and 13 that the triple flame maintains the stabilization process by adjusting its structure to this new and unsteady environment. Also, because of their triple structure, these flames are much more robust than pure non-premixed flames. Indeed, to complete extinction it is required to extinguish both premixed wings and the diffusive part. It has been observed that even when, because of intense vorticity (i.e. strain rate), one of the wings is quenched the others reactive zones are able to sustain the combustion.

From Fig. 13 we observe that the triple-flame is responding to the modification of the chemical species field by a deformation of its internal structure following the location of the stoichiometric value of the mixture fraction. In the case of a single vortex (Fig. 12), the triple point and its wings are convected by the vortex, then eventually the trailing diffusion flame can be locally quenched and a certain amount of premixing is reached. From this local premixed zone, two triple flames facing each other may emerge. During these processes, the local consumption speed of the flame is increased or decreased depending on the position of the vortex with respect to the axis of symmetry.

By inducing a concave shape for the iso-mixture fraction line, a pair of vortices can even reverse the curvature of the wings, as seen in Fig. 13. This "reversible flame" is then convected by the mean velocity of the vortex pair.

When two kernels of premixing are created during the interaction, these two flames propagate, and if in a turbulent environment an iso-stoichiometric line is issued from both of the these premixed flames, two propagating triple-flames will emerge with their trailing diffusion flames.

These observations illustrate how non-premixed combustion can propagate through a turbulent non-uniform mixture, and one may speculate that these generic situations may also be observed in stabilization of turbulent jet flames in open air.

7. Conclusions

Triple flames correspond to the stabilization zone of a diffusion flame between two parallel streams of cold oxidizer and fuel, initially separated by a splitter plate. Such a flame is stabilized in a flow when its propagation speed is able to be sustained by the local flow velocity. As shown from asymptotic theory, two locations where this criterion is satisfied exist. First, the flame may be anchored in the wake of the splitter plate. If the upstream flow velocity is too high, the triple flame may also be lifted and stabilized far from the splitter plate in a zone where the flow velocity is lower. Of course, a too high upstream velocity leads to a complete blow-off of the flame. Numerical simulations of the two situations have been reported and quantitative results have been compared to asymptotic predictions. The flow field upstream of the triple flame is strongly modified by the heat release, and the flame is in fact able to sustain higher free-stream velocities than expected. The agreement with asymptotic theory is found to be qualitatively good. Interactions of the triple flame with a pair of vortices have also been studied. These flames are able to sustain strong vortex interactions by modification of its structure. This mechanism allows us to understand how a diffusion flame may be stabilized in a vortex street.

REFERENCES

DOLD, J. W. 1989 Flame propagation in a nonuniform mixture: analysis of a slowly varying triple flame. *Combust. & Flame.* **76,** 71.

DOLD, J. W., HARTLEY, L. J. & GREEN, D. 1991 Dynamics of laminar triple-flamelet structures in non-premixed turbulent combustion. *Dynamical Issues in Combustion Theory.* Springer-Verlag, 83.

HARTLEY, L. J. & DOLD, W. 1991 Flame propagation in a nonuniform mixture: analysis of a propagating triple-flame. *Combust. Sci. & Tech.* **80,** 23.

KERSTEIN, A. R., ASHURST, WM. T., & WILLIAMS, A. 1988 Field equations for interface propagation in an unsteady homogeneous flow field. *Phys. Rev. A.* **37,** 2728.

KIONI, P. N., ROGG, B., BRAY, K. N. C. & LIÑÁN, A. 1993 Flame spread in laminar mixing layers: the triple flame. *Combust. & Flame.* **95,** 276.

LELE, S. 1992 Compact finite difference schemes with spectral-like resolution. *J. Comp. Phys.* **103,** 16.

LIÑÁN, A. 1974 The asymptotic structure of counterflow diffusion flames for large activation energies. *Acta Astronaitica.* **1,** 1007.

LIÑÁN, A. 1994 Ignition and flame spread in laminar mixing layers. *Combustion in high speed flows.* ed. Buckmaster, Jackson, and Kumar. Kluwer Acad. Pub., 461.

LIÑÁN, A. 1988 Diffusion flame attachment and flame front propagation along mixing layers. *Combust. Sci. & Tech.* **57,** 129.

LIÑÁN, A. & CRESPO, A. 1976 Asymptotic analysis of unsteady diffusion flames for large activation energies. *Combust. Sci. & Tech.* **14,** 95.

POINSOT, T., VEYNANTE, D., & CANDEL, S. 1991 Quenching processes and premixed turbulent combustion diagrams. *J. Fluid Mech.* **228,** 561.

POINSOT, T. & LELE, S. 1992 Boundary conditions for direct simulations of compressible viscous flows. *J. Comp. Phys.* **101,** 104.

RÉVEILLON, J., DOMINGO, P., & VERVISCH, L. 1994 Autoignition in non-uniform mixture. To be published.

ROBERTS, W. L., DRISCOLL, J. F., DRAKE, M. C. & GOSS, L. P. 1993 Images of the quenching of a flame by a vortex – to quantify regions of turbulent combustion. *Combust. & Flame.* **94,** 58.

SAMANIEGO, J. M. 1993 Stretched induced quenching in flame-vortex interactions. *Annual Research Briefs.* Center for Turbulence Research, NASA Ames/Stanford U. 219.

TAKAHASI, F. & SCHMOLL, W. J. 1990 Lifting criteria of jet diffusion flames. *23rd Symposium (International) on Combustion.* The Combustion Institute, Pittsburgh, 677.

VERVISCH, L., KOLLMANN, W., & BRAY K. N. C. 1994 Pdf modeling for premixed turbulent combustion based on the properties of iso-concentration surfaces. *Proceedings of the 1994 Summer Program.* Center for Turbulence Research, NASA Ames/Stanford Univ.

WRAY, A. A. Private communication.